Potential energy landscape and mechanisms of diffusion in liquids

T. Keyes and J. Chowdhary
Department of Chemistry, Boston University, Boston, Massachusetts 02215
(Received 6 September 2001; published 3 April 2002)

The mechanism of diffusion in supercooled liquids is investigated from the potential energy landscape point of view, with emphasis on the crossover from high- to low-T dynamics over the range $T_A \geqslant T \geqslant T_c$. Molecular dynamics simulations with a time dependent mapping to the associated local mininum or inherent structure (IS) are performed on unit-density Lennard-Jones. Dynamical quantities introduced include $r2_{is}(t)$, the mean-square displacement (MSD) within a basin of attraction of an IS, $R2(t)$, the MSD of the IS itself, and $g(t)$, the distribution of IS waiting times. The configuration space is treated as a composite of the contributions of cooperative local regions, and a method is given to obtain the physically meaningful $g_{loc}(t)$ and mean waiting time τ_{loc} from $g(t)$. An understanding of the crossover is obtained in terms of $r2_{is}(t)$ and τ_{loc}. At intermediate T, $r2_{is}(t)$ possesses an interval of linear t dependence allowing calculation of an intrabasin diffusion constant D_{is}. Near T_c, where intrabasin diffusion is well established for $t < \tau_{loc}$, diffusion is intrabasin dominated with $D = D_{is}$; D may be calculated within a basin. Below T_c, τ_{loc} exceeds the time τ_{pl} needed for the system to explore the basin, indicating the action of barriers at the border; $\tau_{loc} = \tau_{pl}$ is a criterion for transition to activated hopping. Intrabasin diffusion provides a means of confinement not involving barriers and plays a key role in the dynamics above T_c. The distinction is discussed between motion among the IS (IS dynamics) below T_c and saddle or border dynamics above T_c, where the system is always close to one of the saddle barriers connecting the basins and IS boundaries are closely spaced and easily crossed. A border index is introduced based upon the relation of $R2(t)$ to the conventional MSD, and shown to vanish at $T \sim T_c$. It is proposed that intrabasin diffusion is a manifestation of saddle dynamics.

DOI: 10.1103/PhysRevE.65.041106 PACS number(s): 05.40.−a, 66.10.Cb, 64.70.Pf

I. INTRODUCTION: DIFFUSION AND THE POTENTIAL ENERGY LANDSCAPE

Knowledge of the physical mechanism of diffusion is essential to an understanding of the dynamical complexities of supercooled liquids. A mechanism should include the collective motions composing the elementary diffusive step, any correlations among the steps, and a statement about whether barrier crossing is important. If so, distributions of barrier heights, ''reaction coordinates'' for barrier crossing, and details of the relevant saddle barriers are significant. Valuable information is encoded in the T dependence of the self-diffusion coefficient D and of the viscosity η (the Stokes-Einstein law $D \sim T/\eta$ holds until very close to the glass transition at T_g). For most normal liquids D exhibits Arrhenius T dependence. In strong liquids [1], this continues all the way down to T_g, while super-Arrhenius behavior, with the apparent activation energy $E_A(T)$ increasing with decreasing T, sets in before T_g in fragile liquids [1]. Some exceptions classified as ''weak'' by Ferrer *et al.* [2], including simple atomic models such as the Lennard-Jones (LJ), show a normal or upper supercooled range of power-law $D(T)$. Clearly the mechanism of diffusion is T dependent, and a straightforward conclusion is that activated potential energy barrier crossing, or *hopping*, plays an important role. In contrast to chemical reactions where the Arrhenius law was first introduced, however, the barriers and reaction coordinates for diffusion have proved elusive. To further complicate matters, free energy or ''entropic'' barriers, associated with the difficulty of finding a low-energy pathway, may also be important. It is not straightforward to infer a mechanism from $D(T)$, and thus there has been considerable speculation.

Adam and Gibbs suggested [3] that liquids may be decomposed into roughly independent cooperatively rearranging regions (CRR) containing z^* particles, with super-Arrhenius behavior arising from the growth of the CRR, and thus the activation free energy, with decreasing T. An influential paper by Goldstein [4] formulated the dynamics in terms of the $3N$-dimensional potential energy U surface, or landscape. He proposed the existence of distinct high- and low-T dynamical regimes, separated by a crossover temperature. At low T the system stays for times long compared to a vibrational period in the basins associated with the local minima of the landscape, and diffusion is governed by infrequent hopping of the saddle barriers connecting adjoining basins. Perhaps the rearrangements of the CRR correspond to reaction coordinates on the landscape. At high T a different, freer motion is presumed to occur. The onset of the low-T mechanism is sometimes described as a transition to hopping, but if the high-T diffusion constant is Arrhenius type, implying activation, the change must be more subtle. The idea of a crossover is central to current thinking about supercooled liquids. We will pursue the landscape point of view in this paper, so the mechanism of diffusion is naturally discussed in terms of the topology.

Goldstein's picture has been extended to involve two characteristic temperatures, meaning that the mechanism changes gradually over a crossover range $T_A \geqslant T \geqslant T_c$. Interesting features of supercooled dynamics such as super-Arrhenius behavior and stretched exponential decay of time correlations first appear at T_A [5] and $D(T)$ extrapolates to zero from above, via a power-law fit, at the mode-coupling temperature $T_c < T_A$ [6]. Note that T_c, defined by the extrapolation, seems a useful quantity regardless of the validity

of mode-coupling theory. An alternative formulation, the ''frustration limited domain'' theory of Kivelson and coworkers [7], introduces an upper crossover temperature T^* at which the collective dynamics first becomes important. Still lower lie T_g, the Kauzmann temperature T_K, and the VTF T_0 [1,2], but this paper is concerned with temperatures from T_A to somewhat under T_c. It is difficult to obtain well-equilibrated computer simulation data below T_c, and impossible to approach T_g.

Stillinger and Weber [8,9] showed how to obtain an explicit description of motion over the landscape in a molecular dynamics simulation, by mapping a $3N$-dimensional liquid configuration $\mathbf{r}(t)$ to the associated minimum $\mathbf{R}(t)$, or inherent structure (IS), with frequent steepest-descent minimizations (faster conjugate-gradient minimizations are equivalent [10] at supercooled T). The configuration space is thus partitioned into the basins of attraction of the IS and the rate of inherent structure transitions (IST) may be measured. The IS mapping is a powerful technique for the investigation of supercooled dynamics but it has not yet been exploited to anything like its full potential. Sastry *et al.* [11] demonstrated in the LJ mixture that the averaged IS energy $\langle U_{is}(T)\rangle$ undergoes a sharp drop (the ''slope'' [5]) from an upper high-T to a lower low-T plateau. They identify the beginning of the drop with T_A, and T_c lies near the apparent bottom. The bottom energy is cooling-rate dependent and the true value, requiring cooling slow enough to maintain equilibration, remains unknown. It is appealing, within the landscape point of view, to relate the change in dynamical mechanism to occupation by the system of lower-lying IS.

More direct investigations of the influence of the landscape on dynamics are possible. The minima of the squared potential gradient $W\equiv|\nabla U|^2$ include all the extrema, or critical points, of U, including minima of order $K=0$ and saddles of order $K>0$. Minimizing W defines a mapping to a configuration which need not be a minimum of U. With critical point mapping, Cavagna [12] Angelani *et al.* [13] showed that minima dominate below T_c, and saddles above. The IS mapping assigns the system to a minimum even if it is in the upper reaches of the basin near the saddle barriers; the critical point mapping does so only if it is actually close to the IS. These authors suggest [12,13] that the crossover is from motion among the minima (IS dynamics) at $T<T_c$ to motion among the saddles (saddle dynamics) at $T>T_c$. Either mapping may be used at any T. Reference to saddle dynamics or IS dynamics below indicates that it gives the simpler, more physical description. The saddle ruled regime [12] is also one of border dynamics. Reaction coordinates leading to several different IS intersect at a multidimensional or ''monkey'' saddle [8], so IS boundaries are closely spaced in the vicinity of a saddle. The system is always near a border, crossings are facile and frequent, and IST are not hops but merely unphysical ''bookkeeping'' events [10]. A much better understanding of the $T>T_c$ region is being achieved with these ideas about saddles and border dynamics.

Recently [10], we gave the first quantitative expression for D in terms of the IST rate $\langle\omega_{is}\rangle$ and the mean-square separation of successive IS. We argued that the long-time slope of the mean-square displacement (MSD) per degree of freedom of the IS configuration, $R2(t)\equiv\langle[\Delta\mathbf{R}(t)]^2\rangle/6N$, is equal to D, as it is for the ordinary MSD $r2(t)$. The IS displacement is the sum of the IST vectors (separations of successive minima) $\Delta\mathbf{R}(t)=\Sigma_{\alpha=1}^{n(t)}\delta\mathbf{R}_\alpha$ after $n(t)$ transitions in time t; for any quantity x, the displacement $\Delta x(t)\equiv x(t)-x(0)$. A key quantity in this approach is the IST vector correlation $C(\beta)\equiv\langle(\delta\mathbf{R}_\alpha\cdot\delta\mathbf{R}_{\alpha+\beta})\omega_{is}\rangle$ [10]. In unit-density LJ, $N=32$ atoms, where $T_c=0.52$ (LJ units), an IST Markov approximation of random walking among the IS predicts D accurately for $T<T_c$ and substantially overestimates D for $T>T_c$. The Markov approximation is equivalent to the statement that the IST vectors are uncorrelated, $C(\beta)=0$, $\beta>0$. Our result supports the idea of long sojourns in the basins below T_c, since the system then has time to lose correlation or memory between IST, leading to a random walk. Because of the uniquely weak T dependence of D at $T>T_c$ in LJ, the transition to hopping may actually be an accurate description of the crossover in this case. The overestimate of D by the Markov approximation at $T>T_c$ is associated with a long-ranged anticorrelation of successive transition vectors, negative $C(\beta)$ at large β, necessary for frequent IST to result in relatively little displacement [10]. *Anticorrelated IST vectors are a signature of the "bookkeeping" IST occurring in border dynamics.*

A problem arises in trying to learn about landscape dynamics with the IS mapping. In the absence of long-range correlations the configuration space of the liquid should be regarded as a composite of the spaces of N_{crr} independent local regions of $z^*\sim O(1)$ particles. A simple model uses $3N$ sinusoidal potentials [14]. Local regions and Adam-Gibbs CRR [3] need not be equivalent, but we will treat them as such. With independent IST occurring in each region, and with a transition for the whole system recorded when any region changes, $\langle\omega_{is}\rangle\sim O(N)$, and the distribution of waiting times between IST, $g(t)$, is correspondingly [8] and unphysically skewed toward short times $\sim O(1/N)$. Computational constraints then indicate that one should simulate the smallest realistic system; with sufficiently large N an IST will be observed on every time step and no meaningful calculation will be possible. More fundamentally, the desired properties are those of the CRR, the building blocks of the macroscopic liquid, but straightforward simulation yields those of the homogenized composite. With increasing N the former become more difficult to disentangle from the latter. This is also true for static quantities. For example, whatever the distribution of U_{is} in a local region, it will be Gaussian for the entire system at large N. Even for the best choice of N some different theory is required to interpret the simulation data.

In this article we further examine the T-dependent mechanism of diffusion in unit-density LJ, $N=32$, via three landscape dynamical entities, and with an initial attempt to derive local relaxation from simulated composite dynamics. The first is $r2_{is}(t)\equiv\langle[\Delta\mathbf{r}(t)]_{is}^2\rangle/6N$, the MSD with no contribution from IST. Starting in a thermal ensemble of basins, $r2_{is}(t)$ is calculated from only those trajectories that remain in the initial basin at time t. The second is $R2(t)$ and the third is the distribution $g_{loc}(t)$ of waiting times in an IS for a local region or CRR. We present a simple method to obtain

$g_{loc}(t)$ from $g(t)$ and N_{crr}, estimated from the averaged participation ratio $\langle P \rangle$ of the IST vectors. The number of degrees of freedom (not particles) participating in an IST is roughly $\langle P \rangle$; thus $z^* \approx \langle P \rangle/3$ and $N_{crr} \approx 3N/\langle P \rangle$.

Comparison of $r2_{is}(t)$, $R2(t)$, $r2(t)$, and $g_{loc}(t)$ casts considerable light upon the relation of diffusion to the landscape. For $t \gg \tau_{pl}$, where τ_{pl} is a characteristic plateau time, $r2_{is}(t)$ attains a constant value, due to the finite volume of the basin [15]. This is true even at high T where the system moves freely among the IS, since only trajectories that remain in the original IS contribute (and thus averaging is difficult). At $T=1.10$ the plateau is reached quickly but a small interval of linear t dependence is visible at intermediate times, from which an intrabasin diffusion coefficient D_{is} may be calculated. Below $T_A \approx 1.0$ the diffusive interval in $r2_{is}(t)$ expands; T_A is estimated as the top of the slope in $\langle U_{is}(T) \rangle$. More cooling reveals that the $T \sim T_c$ regime is intrabasin dominated with $D=D_{is}$—the true diffusion constant may be calculated in a single basin. Thus, as for high T, diffusion cannot consist of a sequence of activated IST hops, but the mechanism is quite different from the high-T mechanism. Intrabasin diffusion arises from the roughness of the landscape at the upper elevations of a basin and provides a mechanism for confinement different from interbasin barriers but nonetheless capable of producing a Markov chain of IST under the right conditions [10]. We suggest that the elementary steps in this process are transitions among the domains of the saddles connected to the IS, i.e., intrabasin diffusion is saddle dynamics. Intrabasin dominated diffusion is also IS dynamics, since the motion among the IS is then a simple random walk; at intermediate T both descriptions are appropriate.

The system does not sense the finite size of the basin until the mean local waiting time τ_{loc} reaches τ_{pl}. We thus have a criterion for the onset of the low-T IS dynamics mechanism and, indeed, it is found that τ_{loc} crosses τ_{pl} slightly below T_c. The analysis would make no sense with an N-dependent mean time taken from $g(t)$. More information is obtained by comparison of $R2(t)$ with $r2(t)$. Let $\mathbf{r}(t)=\mathbf{R}(t)+\mathbf{u}(t)$, where $\mathbf{u}(t)$ is the return vector, the separation of the system from its IS [15]. If $\Delta\mathbf{R}$ and $\Delta\mathbf{u}$ are uncorrelated, $r2(t)$ must lie above $R2(t)$. This is so at low T but as T increases $R2(t)$ rises above $r2(t)$. The relation of $R2(t)$ to $r2(t)$, indicating the correlation of $\Delta\mathbf{R}$ and $\Delta\mathbf{u}$, yields a border index $B(T)$, which complements the information contained in $C(\beta)$ regarding IS vs saddle dynamics. In sum, with some additional applications of the IS mapping we achieve an extremely detailed description of the T-dependent mechanism of diffusion.

II. SIMULATION METHODS

Molecular dynamics simulations are performed on unit-density supercooled LJ [10,16,17], $N=32$, with the methods described in Ref. [10]. As discussed there, and above, a small system should be used for IST dynamics. Increasing N beyond the number required to ''solvate'' a CRR merely creates an intractably large IST rate and makes it difficult to extract the properties of a CRR from those of the composite landscape. Is $N=32$ large enough? The diffusion constants are close to those for $N=108$ [17] and $N=256$ [16], with slightly weaker T dependence. The crystal melts at $T_m \sim 1.6$ and fitting $D(T)$ yields $T_c=0.52$ [10], while at $N=256$ $T_m \sim 1.8$ [16] and (for ''modified'' LJ) $T_c=0.475$ [13]. The saddle order $K(T)$ [12,13] extrapolates to zero at T_c [18] [from $D(T)$ by definition], as is so for $N=108$ [17] and for modified LJ, $N=256$ [13]. The plot of $\langle U_{is}(T) \rangle$ [10] is similar to that of Ref. [13], reaching the ''bottom'' of the landscape at the same $T \approx 0.50$, and with the gentler drop from the high-T plateau expected for small N. Clearly, the essential physical features of the crossover—we make no claim about deeply supercooled liquids—are present at $N=32$ and using a larger system would simply fine-tune various numerical estimates at enormous computational cost [10].

Natural LJ units will be used throughout. Rather than making a single long molecular dynamics run in the supercooled liquid, we average all calculated quantities over an ensemble of quenches, starting from different high $T=5.00$ configurations, to avoid broken ergodicity [19]. The hot liquid is cooled in one step to a temperature in the 1.20–0.60 range. The system is equilibrated for $2.5\tau_{LJ}$, data are gathered for $62.5\tau_{LJ}$, T is decreased by 0.02, and the process is repeated 10–25 times, generating a single quench run; most quenches sampled 16 T. The cooling rate is 3.08×10^{-4}. Sastry *et al.* [11] found in a LJ mixture that quenches with a cooling rate of 2.70×10^{-4}, close to ours, exhibited $\sim 75\%$ of the fall in $\langle U_{is}(T) \rangle$ attained by quenching almost 100 times slower, and reached an apparent bottom somewhat below T_c; this should be adequate for probing the crossover. At $N=32$ the abrupt decreases in U signaling solidification, common at $N=256$, do not occur but some quenches develop solidlike pair distributions and these are discarded. Results are averaged over 23 quenches at the lowest T and 30 at the highest. Quench-to-quench fluctuations are much larger than any systematic changes over $T=0.02$, so we also average results at each T with those from the next higher and lower T. Even so our data are somewhat noisy but the trends are clear for $1.10 \geqslant T \geqslant 0.34$, encompassing the crossover range T_A $(\approx 1.0) \geqslant T \geqslant T_c$ $(=0.52)$. We believe that our results are well averaged and equilibrated down to $\sim T_c$, and are out of equilibrium (but ''well averaged'' over the set of nonequilibrium configurations allowed by the quench) at the lowest T.

Conjugate-gradient minimizations are performed every five time steps $(dt=0.001\,25)$, or 160 minimizations per τ_{LJ}. Since the range of $\langle \omega_{is}(T) \rangle$ is from 9.0 IST per τ_{LJ} at $T=1.10$ to 0.23 at $T=0.34$, this is sufficient. The equivalence of conjugate-gradient and steepest-descent minimizations for the relevant T was verified. The distribution of IST vector (logarithmic) lengths d is bimodal, and to avoid counting contributions of two-level systems and anharmonicities irrelevant to diffusion we record a transition for d in the large-displacement lobe only [20]. Similar considerations have entered the efforts to relate D to $\mathrm{Im}-\omega$ instantaneous normal modes, where nondiffusive modes must be discarded [21].

At each T we obtain the three MSD $r2_{is}(t)$, $R2(t)$, and

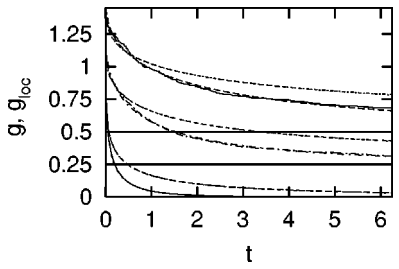

FIG. 1. Composite and local waiting time distribution pairs $g(t)$ and $g_{loc}(t)$ with overlapping KWW fits at $T=0.34$, 0.50, and 1.00, top to bottom. Curves are set to unity at $t=0$, shifted for display, and decay to zero at the horizontal lines; local distribution has slower decay.

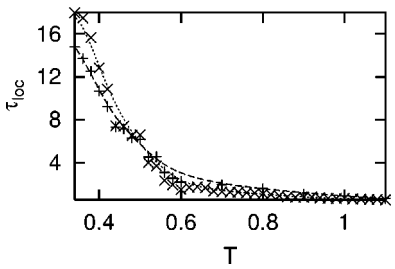

FIG. 2. T dependence of local waiting time from g_{loc} (+) and from $N_{crr}/\langle\omega_{is}\rangle$ (×); smooth curves are spline fits.

$r2(t)$ (yielding D), the distribution of waiting times $g(t)$, and the averaged participation ratio $\langle P\rangle$ of the IST vectors. With the t-dependent IS in hand, evaluation of $R2(t)$ and $\langle P\rangle$ is straightforward. The intrabasin MSD $r2_{is}(t)$ is found from an ordinary MSD algorithm with the condition that, when an IST is detected, the current run is terminated and a new run is begun (new origin of coordinates, MSD$=0$). Binning the times spent in an IS, instead of simply calculating the averaged IST rate, is all that is required for $g(t)$.

III. LANDSCAPE DYNAMICAL PROPERTIES

A. Intra- and interbasin dynamics

Distributions of IS waiting times $g(t)$ are described very well by a KWW (stretched exponential) function $\exp[-(t/\tau)^{\beta}]$ over the entire temperature range. The KWW fit is superior to a sum of two exponentials, even though the latter has one more adjustable parameter. The average $\beta=0.50$, and deviations appear to be noise with no systematic T dependence. To investigate trends in β over a broader T range we obtained data at normal liquid $T=2.00$ and also found, to our surprise, $\beta=0.50$.

One hesitates to read very much into the intriguing half-integral value of β because $g(t)$ is a composite property, dependent upon N_{crr}. An estimate of $g_{loc}(t)$ may be obtained as follows. The probability that there is no IST in time t is $P_{no}(t)=\int_t^{\infty}dt'g(t')$. In a composite, no transition means that no CRR has a transition, and $P_{no}(t)=[\int_t^{\infty}dt'g_{loc}(t')]^{N_{crr}}$. Equating the two expressions, solving for $\int_t^{\infty}dt'g_{loc}(t')$, and taking d/dt yields

$$g_{loc}(t)=\frac{g(t)}{N_{crr}[\int_t^{\infty}dt'g(t')]^{(1-1/N_{crr})}}. \tag{1}$$

The averaged participation ratio of the IST vectors is nearly constant, fluctuating between 19 and 22 over the T range with an average of 21 for $z^*=7.0$ atoms in a CRR and $N_{crr}=4.6$ CRR in the simulation box. Using the average N_{crr} at all T we calculate g_{loc}, which is also well described by a KWW form, with T-independent $\beta=0.36$. Some representative $g_{loc}(t)$ from Eq. (1), simulated $g(t)$, and fits with $\beta=0.36$, and $\beta=0.50$, respectively, are presented in Fig. 1. The shift of $g_{loc}(t)$ to longer times is evident. Processes with KWW distributions are not well characterized by a single time, but the best compromise is the correlation time $\tau_{loc}=\int_0^{\infty}dtg_{loc}(t)/g_{loc}(0)$. Figure 2 provides further evidence [10,17,13] that the low-T diffusive mechanism sets in at $T\sim0.50$, where $\tau_{loc}(T)$ begins to increase strongly. Also shown is $N_{crr}/\langle\omega_{is}\rangle$, the obvious intensive ''composite corrected'' time available from the average IST rate, in reasonable agreement with $\tau_{loc}(T)$.

Let us now view the changes in the mechanism of diffusion with decreasing T through the paired conventional and intra-IS MSD $r2(t)$ and $r2_{is}(t)$, combined with our knowledge of $\tau_{loc}(T)$. The $T\sim T_A$ scenario is found at $T=1.10$, Fig. 3, a relatively high (although supercooled) temperature $\sim 2T_c$ where thermal energy is sufficient for the system to move freely among closely spaced IS borders. The unconstrained MSD diverges from $r2_{is}(t)$ at $t\sim0.36$, before it has even fully established its linear diffusive form. For the same reason the trajectories that stay in the basin explore it quickly; the short-time rise in $r2_{is}(t)$ bends over to form a plateau at about $\tau_{pl}\sim2.0$ with only a glimpse of intermediate-t behavior. Even so, almost all trajectories leave the basin before its finite size is felt, with $\tau_{loc}=0.68\ll\tau_{pl}$ [thus $r2_{is}(t)$ is noisy at long times]. This is illustrated with the inclusion of g_{loc}, scaled to intersect $r2_{is}(t)$ at τ_{loc}. The IST are ''bookkeeping'' events as border dynamics prevails, D is not proportional to $\langle\omega_{is}\rangle$ [10], there is no effective barrier to leaving a basin, and hopping is surely not an apt description. One might say either that intrabasin dynamics are irrelevant to diffusion, or that no distinction exists between interbasin and intrabasin dynamics.

At $T=0.80<T_A$, $r2_{is}(t)$ looks rather different—the diffusive interval has grown to the point that it resembles a conventional MSD and easily allows estimation of an intrabasin D_{is} (see Fig. 4). The plateau must be reached eventu-

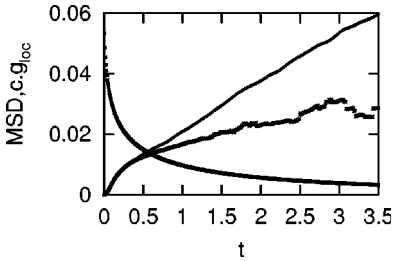

FIG. 3. Conventional (upper) and intrabasin MSD at $T=1.10$. Decaying curve is distribution of local waiting times, scaled to cross the intra-MSD at τ_{loc}. Plots are closely spaced data points.

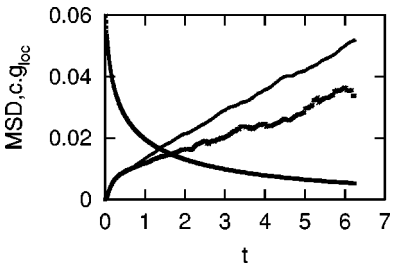

FIG. 4. Same as Fig. 3 for $T=0.80$.

ally, but in the current simulation all we can say is $\tau_{pl} > 6.25$. Comparison with $r2(t)$ shows (Fig. 7) that $D_{is} < D$, with $D_{is}=0.0045$, $D=0.007\,14$. The two MSD have a brief interval of overlap at the beginning of their linear regimes but soon diverge, so the mechanism is not governed by intrabasin diffusion and is probably unchanged from $T=1.10$. Nonetheless, we believe that the emergence of intrabasin diffusion is significant and characteristic of the upper crossover regime. Basins are not harmonic away from the minima and apparently below T_A the higher elevations are rough enough to produce diffusion. An equivalent statement is that the process is best viewed as a random walk among the saddles [12,13]. Configurations in the upper part of a basin are closer to the saddles than to the IS and will be assigned accordingly by the critical point mapping. A random walk among saddles connected to a basin will appear as intrabasin diffusion. At this T ordinary diffusion is also saddle dynamics, so with $D_{is} < D$ it follows that unconstrained saddle dynamics is faster than intrabasin saddle dynamics. The need to utilize an inefficient random walk to escape the basin, and of course the lower thermal energy, has caused the plateau time to increase significantly from its $T=1.10$ value and $\tau_{loc} \ll \tau_{pl}$ holds even more strongly despite an increase in τ_{loc}.

In our picture of intrabasin diffusion, saddle transitions occur while the IS does not change. We previously discussed ''bookkeeping'' IST, where the IS changes but there is little actual motion. With several IS available from a saddle, motion about the basin of attraction of a single saddle naturally generates bookkeeping IST; the IS changes but the saddle does not. Both possibilities, which coexist at intermediate T, may be observed with a time-dependent critical point mapping, made possible by a very efficient algorithm [18]. Figure 5 shows IS and saddle energies vs t at $T=0.70$. In the time interval $0.00 \leqslant t \leqslant 0.70$ the system undergoes seven IS transitions while assigned to the same saddle (bookkeeping IST). For $0.70 \leqslant t \leqslant 1.15$ the IS is constant and there are two saddle transitions at $t \sim 0.8$, followed by rapid exchange between a pair of saddles starting just after $t=1.00$ (intrabasin diffusion).

Cooling to $T=0.50 \sim T_c$ produces a remarkable result. The period of overlapping linear t dependence of $r2_{is}$ and $r2$ is now substantial, and (Fig. 6) the true diffusion constant may be calculated from trajectories with no IST. The system now stays in a basin long enough that on average intrabasin diffusion is fully developed before an IST occurs, and before the plateau is reached (although τ_{loc} is now approaching τ_{pl}; see Fig. 9). Under these circumstances diffusion is intrabasin dominated, and the IST simply act to keep the process going,

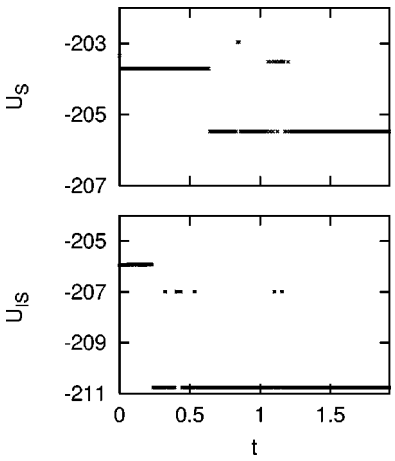

FIG. 5. Saddle (upper) and IS energies vs t; $T=0.70$.

i.e., to avoid the influence of finite basin size. Intrabasin and unconstrained saddle dynamics (ordinary diffusion) are indistinguishable. We have thus some gained perspective on the changes around T_c. There the chain of IST becomes a Markov process [10], and an obvious explanation is that sufficiently long confinement of the system in a basin allows successive IST to lose correlation. While conventionally confinement arises from energy barriers, we find that the system diffuses to the border and crosses with ease. Confinement is produced by diffusion itself; the time required to escape by the random walk is long even absent a barrier at the border. A sufficiently slow walking about the saddles connected to a basin can produce a Markov process among the IS themselves, and IS dynamics is also a good description of the intrabasin dominated regime. Upon close examination, the crossover is not simply from saddle dynamics at high T to IS dynamics at low T. There is a third, intermediate-T region where both descriptions are correct, defined by the condition $D=D_{is}$.

Arrhenius plots of D_{is} and D are displayed in Fig. 7. Estimates of D_{is} are possible for $1.10 \geqslant T \geqslant 0.38$. Linear behavior of $r2_{is}(t)$ is not cleanly visible below $T=0.38$ and is marginal at $T=1.10$; we expect it to disappear at slightly higher T, but collecting data where trajectories leave a basin so quickly is difficult. The intrabasin dominated $D=D_{is}$ range, marked by arrows, is approximately $T_c=0.52 \geqslant T \geqslant 0.46$. Starting from high T, the upper limit of intrabasin dominance is reached when two conditions hold: T is low enough for $r2_{is}(t)$ to have a diffusive t interval, and τ_{loc} adequately exceeds the time at which that interval begins.

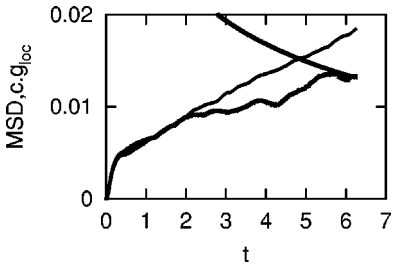

FIG. 6. Same as Fig. 3 for $T=0.50$.

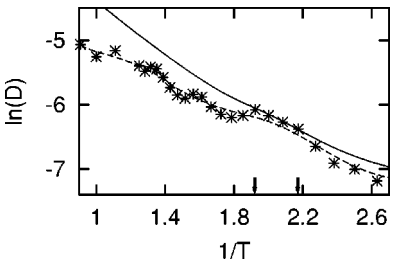

FIG. 7. Natural logarithms of intrabasin diffusion constant D_{is} (dashed line spline fit and points) and true D (solid line) vs $1/T$. Intrabasin dominated $D=D_{is}$ range delimited by arrows; left arrow coincides with T_c.

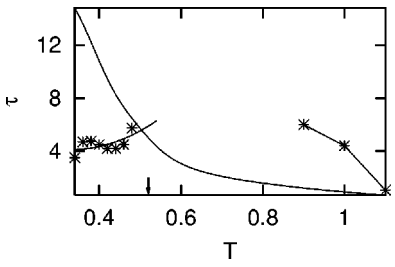

FIG. 9. Local waiting time τ_{loc} and, in two segments (line plus $\star$), rough estimate of plateau time τ_{pl} vs T; low-T data shown with quadratic fit. Arrow indicates T_c.

For the lower limit, either of two conditions may be true: τ_{loc} substantially exceeds τ_{pl}, so a barrier to leaving the basin exists and activation becomes important, or the linear portion of $r2_{is}(t)$ shrinks so that it no longer represents the intrabasin motion. In fact, both appear to set in gradually and simultaneously.

At our lowest temperature, $T=0.34$ (Fig. 8), $r2_{is}(t)$ rises quickly to the plateau just as at the high $T=1.10$; a linear region of this curve cannot be identified and τ_{pl} is now back within the $6.25\tau_{LJ}$ window.

Quantitative estimates of $\tau_{pl}(T)$, along with $\tau_{loc}(T)$, are shown in Fig. 9; at intermediate T all we can say is that $\tau_{pl}>6.25$. While τ_{pl} is short at high T because of the abundant thermal energy, it is short at low T because the system occupies the lower regions of the basin only. Thus (a) the plateau is reached after a shorter displacement, and (b) the intrabasin motion is mostly fast harmonic oscillations, not diffusion. The τ_{pl} and τ_{loc} curves cross at $T\approx 0.51$, and we propose $\tau_{pl}=\tau_{loc}$ as a way to define a crossover temperature. Below $T=0.51$ the system explores the accessible portion of the basin more quickly but exits more slowly, indicating barriers at the border. Gradually, saddle dynamics loses out to IS dynamics as the physical description, $D\neq D_{is}$ below $T=0.46$, and barrier crossings assume the rate-limiting role for diffusion.

In addition to the standard analysis of $D(T)$ and the results of very recent work [13,10,17], we now have two more indicators pointing to a change in the mechanism of diffusion at $T\sim 0.50$. The local waiting time τ_{loc} crosses τ_{pl} at $T=0.51$, and intrabasin dominance sets in at $T=0.52$ with $D=D_{is}$ for $0.52\geqslant T\geqslant 0.46$. However, the crossover develops over a wide temperature range, and involves much more than the presence or absence of hopping, as explained in the last few paragraphs. We hope it is clear that the IS mapping is a powerful tool for studying the dynamical crossover.

B. Landscape vector correlations, saddle dynamics, and borderism

IST vectors are anticorrelated at high T [10], and correlation decreases through the crossover range until the IST Markov approximation becomes accurate below T_c. A substantial negative value of $C(\beta)$ is a sign of saddle or border dynamics, while $C(\beta)\sim 0$ indicates IS or hopping dynamics. IS borders are closely spaced near a multidimensional saddle. Anticorrelation is required for the bookkeeping IST arising from a small motion through such a region not to predict, wrongly, a large motion. This implies that saddle dynamics is a more physical description than IS dynamics. A simple process appears complicated when formulated with inappropriate elementary steps, and loss of correlation signals the onset of the low-T mechanism, which is truly IS dynamics.

Analysis of the MSD within the basin of attraction of an IS, $r2_{is}(t)$, proved quite fruitful. We will now see that such is also the case for the MSD of the IS itself, $R2(t)$, leading to another informative correlation, that of the return vector and the IS configuration. With the definitions from the Introduction,

$$r2(t)=R2(t)+\langle[\Delta\mathbf{u}(t)]^2\rangle/6N+2\langle\Delta\mathbf{R}(t)\cdot\Delta\mathbf{u}(t)\rangle/6N. \tag{2}$$

It follows that $r2(t)\geqslant R2(t)$ unless the IS displacement $\Delta\mathbf{R}(t)$ and the return vector displacement $\Delta\mathbf{u}(t)$ are anticorrelated. Figure 10 shows that at $T=1.00$ $R2(t)$ lies above $r2(t)$, they are nearly superimposed at $T=0.80$, and the ''ob-

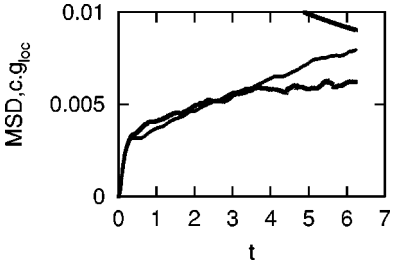

FIG. 8. Same as Fig. 3 for $T=0.34$.

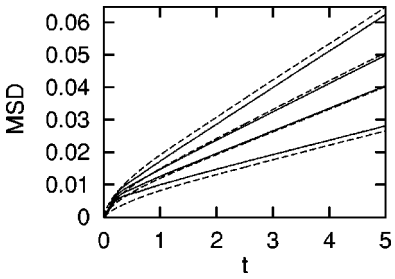

FIG. 10. Ordinary MSD (solid) and IS MSD (dashed) vs t; top to bottom, $T=1.00$, 0.90, 0.80, 0.70.

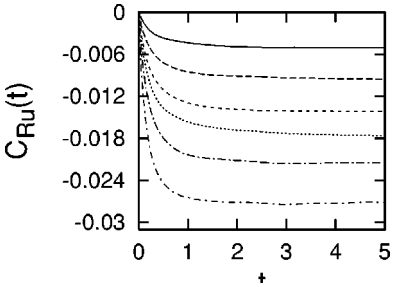

FIG. 11. Correlation $C_{\mathbf{Ru}}(t)$, amplitude increasing with increasing T; top to bottom, $T=0.60$, 0.70, 0.80, 0.90, 1.00, 1.20.

vious'' $r2(t) \geqslant R2(t)$ holds at $T<0.80$. Thus the pattern of anticorrelation of IST vectors $\delta\mathbf{R}_\alpha \cdot \delta\mathbf{R}_{\alpha+\beta}$ at high T, decreasing with decreasing T, is repeated with the $\Delta\mathbf{R}(t)\cdot\Delta\mathbf{u}(t)$ correlation.

For a more quantitative analysis we have calculated $\langle[\Delta\mathbf{u}(t)]^2\rangle$. One anticipates a rapid decay of $\langle\mathbf{u}(t)\cdot\mathbf{u}(0)\rangle$ leading to $\langle[\Delta\mathbf{u}(t)]^2\rangle \rightarrow 2\langle q^2\rangle$, and this expectation is correct. The correlation $C_{\mathbf{Ru}}(t) \equiv \langle\Delta\mathbf{R}(t)\cdot\Delta\mathbf{u}(t)\rangle/6N$, determined from $r2(t)$, $R2(t)$, and $\langle[\Delta\mathbf{u}(t)]^2\rangle$ via Eq. (2), decays quickly (Fig. 11) to an asymptotic negative value which decreases in amplitude with decreasing T. We suggest that $C_{\mathbf{Ru}}$ is a direct measure of the degree of *borderism*—the extent to which the system exists on the IS borders [22].

Expressing $\Delta\mathbf{R}(t)$ as the sum of the IST vectors the most important contributions are evident:

$$6NC_{\mathbf{Ru}}(t) = \langle\delta\mathbf{R}_n\cdot\mathbf{u}(t)\rangle - \langle\delta\mathbf{R}_1\cdot\mathbf{u}(0)\rangle + (\text{smaller terms}). \tag{3}$$

The first term on the right-hand side (RHS) may be understood with Fig. 12, a one-dimensional illustration of the situation at time t, just after the nth IST. The system has moved from the left- to the right-hand basin and it follows that $\delta\mathbf{R}_n$ and $\mathbf{u}(t)$ point in opposite directions, with a negative contribution to $C_{\mathbf{Ru}}$. For the second term on the RHS, set $t=0$ in Fig. 12. The first IST will occur from right to left in the future so change $\delta\mathbf{R}_n$ to $\delta\mathbf{R}_1$ and reverse its direction. The vectors now point in the same direction so with the minus sign in Eq. (3) this contribution to $C_{\mathbf{Ru}}$ is also negative. In the $3N$-dimensional configuration space (or $3N_{crr}$-

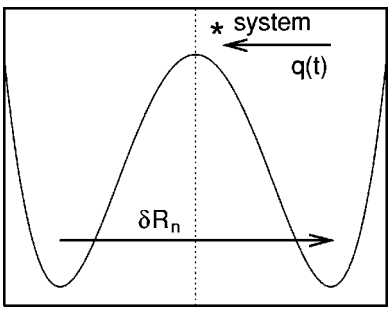

FIG. 12. Return vector $\mathbf{u}(t)$ and IST vector $\delta\mathbf{R}_n$ at time t just after nth (most recent) IST.

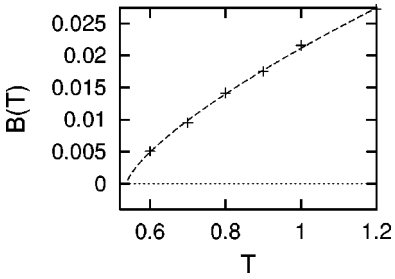

FIG. 13. Border index $B(T)$ (points) and power-law fit, tending to zero at $T=0.53$.

dimensional local region space) the vectors will be distributed about the $d=1$ relative orientations, reducing the dot products.

The geometrical arguments apply when $\mathbf{u}(0)$ is evaluated just before and $\mathbf{u}(t)$ just after an IST. For border dynamics these conditions ''always'' hold and $C_{\mathbf{Ru}}<0$. On the other hand, if the system oscillates about the IS for long periods between IST, the low-T scenario, the return vector has no special relation to any IST vector at any time and $C_{\mathbf{Ru}}\sim 0$. The correlation of $\Delta\mathbf{R}(t)$ and $\Delta\mathbf{u}(t)$ is a maximum for pure border dynamics and vanishes in a hopping model. The interesting part of $C_{\mathbf{Ru}}$ is its asymptotic value and we define

$$B(T) \equiv -C_{\mathbf{Ru}}(\infty, T) \tag{4}$$

as the *border index*. The T dependence of the border index is shown in Fig. 13. It extrapolates to zero via a power-law fit for $1.2 \geqslant T \geqslant 0.60$ at $T=0.53$, yielding another physically appealing route to a crossover temperature. The fit range differs from that used for T_c but $B(T)$ is close enough (power $=0.74$) to linear in T that we expect only a small effect.

IV. DISCUSSION

In the foregoing we have examined the T-dependent physical mechanism of diffusion in unit-density LJ. For some perspectives, it is useful to ask why this is a nontrivial problem. LJ is classified as weak/nonfragile, indicating weak T dependence at high T and a constant activation energy at low T [2]. The simulated diffusion constant is indeed well represented by

$$D(T) = 0.39T\exp(-1.16/T) \tag{5}$$

for $1.10 \geqslant T \geqslant 0.34$; $E_A = 1.16$. The factor of T is appropriate because $D\sim T$ at high T and constant density. Linear or other multiplicative powers are not very important when fitting over several decades but we have only $20\times$ and they significantly influence the goodness of fit and the value obtained for the activation energy. Despite the simplicity of Eq. (5), fitting the same data to a power law for $2.0 \geqslant T \geqslant 0.60$ [18] yields a reasonable T_c [13]. One might well wonder if anything is going on beyond a gradual change from $T \gg E_A$ to $T \ll E_A$. That is, a bare-bones prescription for a transition to hopping, consistent with the IST approaching a Markov chain [10] and the saddle order extrapolating to zero [17,18].

However, it then seems odd that $E_A=1.16$ does not appear as a characteristic dynamical temperature instead of various $T\sim 0.50$, and the sharp drop in $\langle U_{is}(T)\rangle$ around T_c suggests that the crossover is more interesting. To investigate this crucial point we have begun to catalog the saddles and barrier heights in unit-density LJ [18]. Starting from the thermal configuration the IS is determined and the connected first-order saddles are found by eigenmode following [18]. Steepest descent from the saddle yields barrier heights ΔU, which may be collected as a function of IS energy [23] or of the original temperature. Preliminary results [18] are that the barrier heights increase through the slope region [5,11] of $\langle U_{is}(T)\rangle$ from $\langle \Delta U(T=1.20)\rangle=2.8$ to $\langle \Delta U(T=0.40)\rangle=3.7$; T is less than the averaged barrier height for the entire range of this study. The same result has recently been obtained in a soft-sphere mixture [23]. Comparisons of barrier heights to T must be made carefully. Most discussions of barrier crossing assume that ΔU is much greater than T, but that does not apply here, and one might argue that the relevant height is $(\Delta U-T)$. Even with such a modification, average barrier heights remain larger than E_A, indicating—along with the results found above—that the mechanism of diffusion in LJ is highly nontrivial.

There are two explanations for the clear presence of a high-T mechanism with free motion among the basins at $T>T_c$ despite an apparent requirement for activated hopping. One is the broad distribution of barrier heights, reflected in the low $\beta=0.36$ for the KWW distribution of local waiting times. Even if T falls below $\langle \Delta U(T)\rangle$, there will be no transition to low-T dynamics if enough low barriers remain. The average alone does not adequately describe the physics. Furthermore, there are several ways to perform the average [18] and a physically motivated choice must be made. For example, a calculation of $\langle \Delta U(T)\rangle$ including saddles of all orders would be nonsense, since high barriers that are never visited in thermal motion would dominate. Averaging over first-order saddles eliminates many irrelevant high barriers, but not necessarily all. Other topological features such as the connectivity of the IS and saddles should be important as well. The landscape determines T_c and more generally $D(T)$ through the interplay of several physically significant effects. Note that one important landscape quantity, $\langle U_{is}(T)\rangle$, is a ''thermodynamic'' property of the basins. One can imagine different liquids with the same $\langle U_{is}(T)\rangle$ and different T-dependent distributions of barrier heights, giving rise to quite different activation energies and other aspects of dynamics.

Another explanation is found in Cavagna and co-workers' [12,23] argument that barrriers are irrelevant while the saddle mechanism dominates, so the action of a high-T mechanism while T is less than $\langle \Delta U\rangle$ need present no conundrum. Then, when the saddle mechanism shuts down and activation becomes required at $T\sim 0.50$, the barrier heights have already completed most of their growth. The system will exhibit approximate Arrhenius behavior upon further cooling. Cavagna gives a ''fragile'' scenario where the barriers are already much greater than T at T_c, for a very strong increase in relaxation time. However, although we have $\langle \Delta U(T_c)\rangle/T_c\sim 6$, E_A is only $\sim 2T_c$, presumably due to the importance of low-barrier paths. Relatively weak Arrhenius behavior at $T\leqslant T_c$ results, consistent with LJ being a weak or nonfragile liquid [2].

Even if $E_A=1.16$ is not meaningful at higher T, Eq. (5) can still fit the data because the Arrhenius factor is approaching its E_A-independent high-T limit. Saddle dynamics, in which $D(T)$ is proportional to the number of $\mathrm{Im}-\omega$ instantaneous normal modes or [21] the saddle order $\langle K(T)\rangle$ [17], apparently is consistent with $D\sim T$. Thus Eq. (5) can represent the full T range, but the empirical activation energy is a compromise resulting from the fitting process with no simple relation to a barrier height.

In either case the crossover is seen to be a subtle, complex process. Application of the IS mapping has revealed far more than could be deduced from $D(T)$ alone, including (1) intrabasin and intrabasin *dominated* diffusion, associated with saddle dynamics; (2) the distribution of local waiting times, well behaved as $N\rightarrow\infty$, calculated from the simulated distribution with the idea that the configuration space is a composite; (3) a physically appealing criterion for dynamical crossover, $\tau_{loc}=\tau_{pl}$; (4) a quantitative indicator $B(T)$ of the dominance of saddle or border dynamics (borderism), which also yields a crossover temperature.

The value of $T_c=0.52$, from a power-law fit to $D(T)$, is now just one of many pieces of evidence that a dynamical crossover occurs at $T\sim 0.50$. From recent prior work [10,17] we know the following. (1) The IS energy $\langle U_{is}(T)\rangle$ is undergoing its steepest fall. The true bottom is uncertain due to cooling-rate dependence and the steepest fall only identifies the general vicinity of the crossover. (2) The saddle order $K(T)$ also extrapolates to zero at $T=0.52$. (3) The IST Markov approximation becomes accurate at $T\sim T_c$. In this paper we have added the following. (4) $D=D_{is}$, diffusion is intrabasin dominated, for $0.52\geqslant T\geqslant 0.46$. (5) The local waiting time reaches the time taken to explore the basin, $\tau_{loc}=\tau_{pl}$, at $T=0.51$. (6) The border index $B(T)$ extrapolates to zero at $T=0.53$. We suggest that points 3–5 are particularly direct evidence that the mechanism of diffusion is changing. They are based on ideas about the mechanism itself, while a fit to $D(T)$ produces a characteristic temperature based upon the ''symptoms.'' Although points 1–6 focus attention on a narrow range $0.53\geqslant T\geqslant 0.46$, the crossover is gradual and might be thought to take place over $1.10\geqslant T\geqslant 0.38$, the interval where intrabasin diffusion can be detected, encompassing the slope of $\langle U_{is}(T)\rangle$. This agrees roughly with having the crossover begin at T_A.

We believe it is significant that intrabasin diffusion can produce confinement for times long enough that the IST become a Markov chain, without invoking barriers. Thus diffusive confinement and confinement by barriers become two distinct features of the mechanism. Since intrabasin diffusion can be explained as saddle dynamics, our work fits with the growing recognition that the saddles of the landscape need to be considered on an even footing with the IS. There is no contradiction in having the intrabasin diffusion and IST Markov regimes overlap. In the latter case $D\propto\langle\omega_{is}\rangle$, and in the former, since escape from a basin requires diffusion to the border, $\langle\omega_{is}\rangle\propto D_{is}$.

Our simulation model exhibits most of the physical fea-

tures currently being discussed for moderately supercooled dynamics, as well as some additional ones found here. There is much to be learned from a LJ liquid, $N=32$, although of course we intend to apply our methods to other liquids. It is difficult to achieve equilibrium below T_c. Note that, even though we report data down to $T=0.34$, only one significant T appearing in the above estimates is below 0.50, the end of intrabasin dominance at $T=0.46$. Our interest is the cross-over and the lowest, probably nonequilibrated, T are not required for the principal conclusions.

ACKNOWLEDGMENTS

We would like to thank Frank Stillinger for valuable discussions. This work was supported by the NSF through Grant Nos. CHE9708055 and CHE0090975.

[1] C.A. Angell, Science **267**, 1924 (1995).
[2] M. Ferrer, C. Lawrence, B. Demirjian, D. Kivelson, G. Tarjus, and C. Alba-Simionesco, J. Chem. Phys. **108**, 8010 (1998).
[3] G. Adam and J.H. Gibbs, J. Chem. Phys. **43**, 139 (1965).
[4] M. Goldstein, J. Chem. Phys. **51**, 3728 (1969).
[5] C.A. Angell, B. Richards, and V. Velikov, J. Phys.: Condens. Matter **11**, A75 (1999).
[6] W. Goetze and L. Sjogren, Rep. Prog. Phys. **55**, 241 (1992).
[7] P. Viot, G. Tarjus, and D. Kivelson, J. Chem. Phys. **112**, 10 368 (2000).
[8] F.H. Stillinger and T.A. Weber, Phys. Rev. A **28**, 2408 (1983); Science **225**, 983 (1984).
[9] F.H. Stillinger, Science **267**, 1935 (1995).
[10] T. Keyes and J. Chowdhary, Phys. Rev. E **64**, 032201 (2001).
[11] S. Sastry, P. Debenedetti, and F.H. Stillinger, Nature (London) **393**, 554 (1998).
[12] A. Cavagna, Europhys. Lett. **53**, 490 (2001).
[13] L. Angelani, R. Di Leonardo, G. Ruocco, A. Scala, and F. Sciortino, Phys. Rev. Lett. **85**, 5356 (2000).
[14] B. Madan and T. Keyes, J. Chem. Phys. **98**, 3342 (1993).
[15] R. LaViolette and F.H. Stillinger, J. Chem. Phys. **83**, 4079 (1985).
[16] T. Keyes, J. Chem. Phys. **101**, 5081 (1994); Phys. Rev. E **59**, 3207 (1990).
[17] J. Chowdhary and T. Keyes (unpublished).
[18] J. Chowdhary and T. Keyes (unpublished).
[19] D. Frantz, D. Freeman, and J. Doll, J. Chem. Phys. **93**, 2769 (1999); I. Andricioaei and J.E. Straub, *ibid.* **107**, 9117 (1997).
[20] C. Donati, F. Sciortino, and P. Tartaglia, Phys. Rev. Lett. **85**, 1464 (2000).
[21] Wu-Xiong Li and T. Keyes, J. Chem. Phys. **111**, 5503 (1999); E. La Nave, A. Scala, F. Starr, F. Sciortino, and H.E. Stanley, Phys. Rev. Lett. **84**, 4605 (2000).
[22] J. Kurchan and L. Laloux, J. Phys. A **29**, 1929 (1996).
[23] T. Grigera, A. Cavagna, I. Giardina, and G. Parisi (unpublished).